FREQUENCY SCALING OF CATHETER-BASED MAGNETO-INDUCTIVE MR IMAGING DETECTORS

R.R.A.Syms[1], I.R. Young[1], and M.Rea[2]
[1]EEE Dept., Imperial College London, UK
[2]Dept. of Radiology, Imperial College Healthcare NHS Trust, UK

ABSTRACT

Frequency scaling rules are introduced for catheter-based magneto-inductive magnetic resonance imaging detectors, intended for *in vivo* imaging of the vascular and biliary ductal systems. The design is based on a cascade of magnetically coupled L-C resonators, fabricated as a thin-film circuit and mounted on a catheter. Intrinsic safety is introduced using resonant elements designed to avoid coupling to uniform RF magnetic and electric fields. Mapping of reception patterns and high-resolution ^{1}H imaging are demonstrated in a 3 T clinical scanner.

KEYWORDS

MRI, Magneto-inductive wave, Microcoil

INTRODUCTION

Radio frequency (RF) receivers are required for signal detection in magnetic resonance imaging (MRI). Although small resonant coils generally have low quality-factors, a larger filling factor can be obtained from close coupling to the signal source, leading to a greater overall signal-to-noise ratio (SNR) at the price of a reduction in field of view (FOV) [1]. Many small coils have been developed for high-resolution internal imaging of small vessels such as arteries [2] and for catheter tracking [3]. Such coils must be prevented from coupling to the external B_1 field of the transmitter, typically with passive or active diode-switched decoupling. Furthermore, long conductors must be avoided; because of the high RF dielectric constant of tissue [4], even short lengths may be rapidly heated due to standing wave excitation by the E field near transmitter coil capacitors [5]. Proposed solutions include transformer subdivision of cables [6, 7].

We have been developing an alternative based on magneto-inductive (MI) waveguides, linear arrays of magnetically coupled L-C resonators [8]. We have shown that such guides have similar properties to transformer-segmented cable [9], and have demonstrated a low-loss thin-film format [10]. Because the structure is smooth and flexible, it may be wrapped around a catheter scaffold and held in place with heat-shrink tubing (Fig. 1). As a result, it may potentially be applied to many functional catheters, including imaging probes for endoscopic delivery into the biliary ductal system.

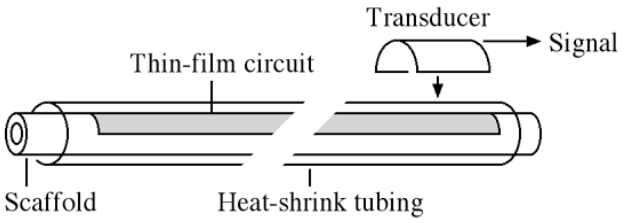

Figure 1: MR-imaging catheter receiver concept.

Operation has been demonstrated in a 1.5 T clinical scanner [11]. Simple scaling rules are needed to adapt the design for higher fields capable of providing increased SNR without expensive iteration. The aim of this paper is to provide such rules and demonstrate imaging at 3 T.

DESIGN AND FREQUENCY SCALING

A magneto-inductive waveguide (Fig. 1) is a linear array of magnetically coupled L-C resonators with angular resonant frequency $\omega_0 = 1/\sqrt{(LC)}$. Assuming internal resistance R, the Q-factor is $Q = \omega_0 L/R$. The resonators are coupled together by a mutual inductance M. As a result, the MI waveguide supports slow waves of circulating current. Propagation loss is minimized by maximizing M and Q, and at resonance the guide has the characteristic impedance $Z_{0M} = \omega_0 M$ [8].

The guide may be coupled to a load with real impedance Z_0 (such as the input of a scanner) using a further magnetically coupled resonant element, which for generality has parameters R', L' and C' such that $1/\sqrt{(L'C')} = \omega_0$ and $Q' = \omega_0 L'/R'$. However, the mutual inductance M' must be slightly different for impedance matching, and standard theory requires that $\omega_0 M' = \sqrt{(Z_0 Z_{0M})}$. Similarly the system may be formed into a resonant receiver by the addition of a similar element acting as a detector. However, the mutual inductance M'' must again be different, and matching is achieved if $\omega_0 M'' = \sqrt{(RZ_{0M})}$.

Precessing nuclear dipoles may induce voltages in any of the loops, allowing the system to detect MRI signals along its entire length. These signals propagate to the load as MI waves [12]. However, sensitivity is highest at the tip, which behaves as a resonant detector.

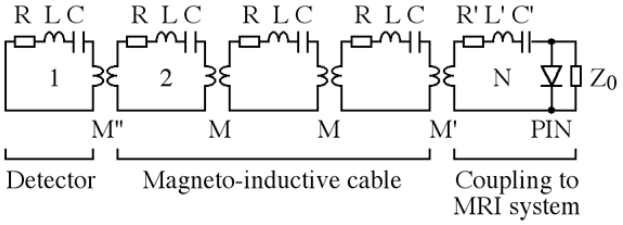

Figure 2: Equivalent circuit of MI receiver.

In MI cable, the resonant elements are formed as thin-film components in copper-clad Kapton (Fig. 3a). The inductors are single-turn loops. A figure-of-eight layout is used to avoid coupling to external B_1 fields, and the element length Λ is taken to be shorter than half a wavelength in a medium with the relative dielectric constant ε_r of tissue to avoid excitation of standing-wave resonances by external E fields. Since $\varepsilon_r \approx 77$ at the frequency of ^{1}H MRI at 1.5 T (63.85 MHz), this length is

around 27 cm. The capacitors are parallel plate structures that use the substrate as an interlayer dielectric, and are split into two components to avoid the need for vias. To minimize width, capacitors are laid alongside inductors.

A cable is constructed by overlaying the adjacent elements to their maximum extent so that the period a is $\approx \Lambda/2$ (Fig. 3b). A receiver is constructed by addition of a detector and a demountable resonant transducer. Impedance matching at the detector is achieved by careful choice of the overlap b, while matching at the transducer is achieved by adjusting the position of a two-turn spiral inductor (which has a large self-inductance L').

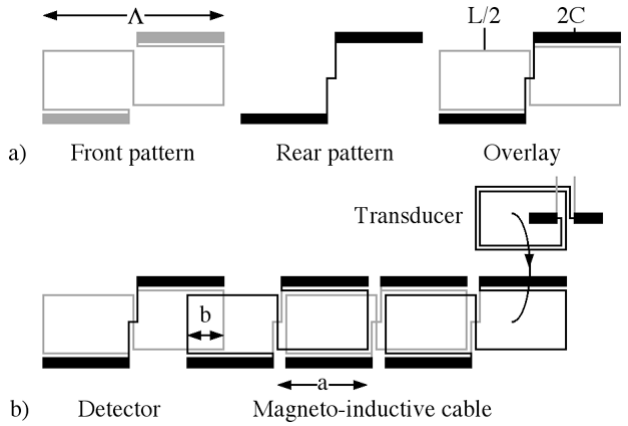

Figure 3: Layout of a) resonant element, and b) receiver.

Scaling rules that allow designs used for one value of static magnetic field B_0 to be adapted for another may be developed as follows. The Larmor frequency scales with B_0. Assuming the dielectric constant of tissue is roughly independent of frequency near 100 MHz, the critical length for standing wave excitation is inversely proportional to frequency, and hence the element length Λ must scale inversely with B_0. In the layout of Fig. 3, many component values are approximately proportional to Λ, and must therefore be inversely proportional to B_0. Conveniently, appropriate scaling of element length then yields the correct resonant frequency automatically, and leaves the characteristic impedance and transducer matching condition unchanged. At low frequency, Q-factor scales with ω_0; however, including the skin effect, Q scales with $\omega_0^{1/2}$. As a result, both Q and the detector matching condition alter slowly with B_0 and Λ. These relations are summarized in Table 1.

Table 1: Scaling of key parameters.

Parameter	Size scaling	Field scaling
R	$[\Lambda]^1$	$[B_0]^{-1}$
L	$[\Lambda]^1$	$[B_0]^{-1}$
C	$[\Lambda]^1$	$[B_0]^{-1}$
M	$[\Lambda]^1$	$[B_0]^{-1}$
L'	$[\Lambda]^1$	$[B_0]^{-1}$
$\omega_0 = 1/\sqrt{(LC)}$	$[\Lambda]^{-1}$	$[B_0]^1$
$Z_{0M} = \omega_0 M$	$[\Lambda]^0$	$[B_0]^0$
$\omega_0 M' = \sqrt{(Z_0 Z_{0M})}$	$[\Lambda]^0$	$[B_0]^0$
$Q = \omega_0 L/R$	$[\Lambda]^{-1}$ - $[\Lambda]^{-1/2}$	$[B_0]^1$ - $[B_0]^{1/2}$
$\omega_0 M'' = \sqrt{(RZ_{0M})}$	$[\Lambda]^{1/2}$ - $[\Lambda]^{1/4}$	$[B_0]^{-1/2}$ - $[B_0]^{-1/4}$

FABRICATION AND MEASUREMENT

Magneto-inductive catheter imaging probes have already been demonstrated at 1.5 T, based on an element length of 20 cm and an inductor width of 3.3 mm (for integration on a 2.2 mm dia scaffold). The implication of Table I is that a design for operation at 3 T may be developed from this by halving resonant element lengths and adjusting the detector position. CAD layouts for resonant elements and transducers were designed using these scaling rules, with Λ = 10 cm and the same inductor width (Fig 4a). Arrays of MI waveguides (Fig. 4b) were fabricated in 1 metre lengths by double sided lithography and etching of copper-clad Kapton (35 µm Cu on 25 µm polyimide), together with separate detector and transducer elements. Guides were separated, the resonant frequency was adjusted by trimming the capacitors, a detector was added, and the circuit was mounted on a catheter scaffold using heat shrink tube (Fig. 4c). Finally, a resonant transducer was mounted in a split Perspex clamp and attached to the cable (Fig. 4d).

Figure 4: a) CAD layout, b) completed cable array, c) catheter mounted cable, d) resonant transducer.

Electrical testing was carried out using an Agilent E5061A network analyzer. Parameters were first extracted from single and paired elements, by using inductive probes for measurement of resonant frequencies with in-built and surface mount capacitors for tuning, as C = 12 pF, L = 130 nH, Q = 70, M = 39 nH, Z_{0M} = 31 Ω, and C' = 6.6 pF, L' = 230 nH, and Q' = 85. The response of complete receivers was then measured, in the latter case using a small loop to couple to the detector. Fig. 5a compares the actual frequency dependence of the reflection (S_{11}) and transmission (S_{21}) of receivers designed for 1.5 T and 3.0 T. In each case the system is impedance matched, and the transmission peaks correctly at resonance, with a loaded Q-factor of ≈ 30.

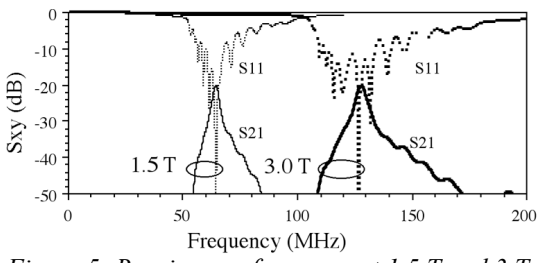

Figure 5: Receiver performance at 1.5 T and 3 T.

When the responses are plotted against normalized frequency (Fig. 6), the results are almost identical, directly validating the scaling rules.

Propagation losses were established from separate measurement of the transmission of a similar MI cable, as ≈ 8 dB. These losses are relatively high, and represent the major current limitation of magneto-inductive receivers.

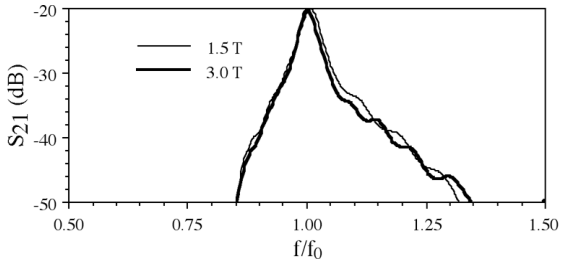

Figure 6: Normalised performance at 1.5 T and 3 T.

MAGNETIC RESONANCE IMAGING

^{1}H magnetic resonance imaging was carried out using a GE Discovery MR750 3 T clinical scanner, with the catheter receiver connected to the auxiliary coil input for signal reception, and a non-magnetic PIN diode connected across the input to enable the receiver to pass the pre-scan impedance test. The catheter was arranged parallel to the magnet bore, near the magnet isocentre. Imaging was carried out using a 2D fast spin echo sequence, with *TE* = 42 msec and *TR* in the range 400 – 1200 msec. Tests were initially carried out in an immersion tank containing a solution of 3.37 g/L $NiCl_2.6H_2O$ and 2.4 g/L NaCl, with *T1* = 500-800 ms and *T2* = 100-200 ms (Fig. 7).

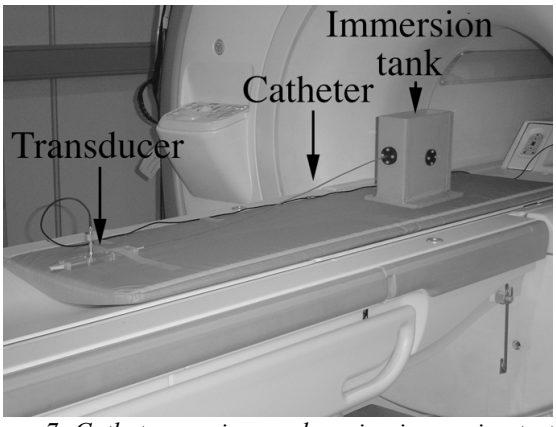

Figure 7: Catheter receiver undergoing immersion test.

Fig. 8a shows an axial slice across the catheter, obtained using the body coil. Here, the bright part of the image corresponds to the immersion liquid. Uniform brightness implies that the figure-of-eight element layout has correctly minimized coupling to the B_1 field during excitation, and hence any perturbation to the local magnetization. Fig. 8b shows the corresponding slice obtained using the catheter receiver. Here, the image is brighter in the immediate vicinity of the catheter, but the brightness falls off rapidly with distance, confirming the limited FOV (ca 20 mm dia) of the catheter receiver. Fig. 8c shows a 3D surface reconstruction obtained from a set of sagittal images, which shows that the reception pattern is multi-lobed, with nulls at the element crossover points.

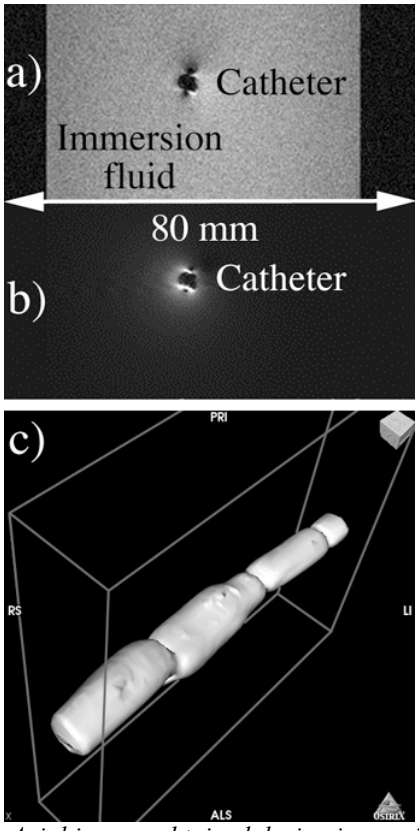

Figure 8: Axial images obtained during immersion testing using a) the body coil and b) the catheter receiver; c) reception pattern reconstructed from sagittal images.

Tests were then carried out with the catheter receiver mounted on a cuboid phantom, initially without and later with an additional resolution test phantom at the tip (Fig. 9). The resolution phantom consisted of a cylindrical container filled with the same tissue-simulating solution, together with an array of small-diameter plastic tubes to give internal structure.

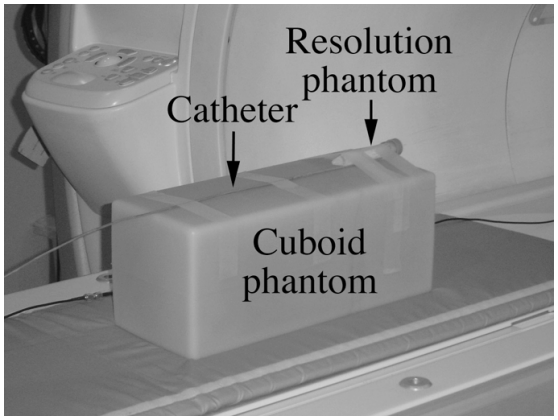

Figure 9: Catheter receiver with test phantoms.

Fig. 10a shows a coronal image obtained using the catheter receiver near the top of the cuboid, without the resolution phantom. An image is clearly obtained along the length of the cuboid, in the immediate vicinity of the catheter. The reception pattern is again multi-lobed, with the two brightest lobes at the bottom corresponding to the catheter tip and the remainder to the MI cable sections leading back to the transducer. Fig. 10b shows a further

surface reconstruction obtained from the entire stack of coronal images, which define the reception pattern in three-dimensional space. Some curvature of the FOV can be seen, which lies outside the region of gradient linearity.

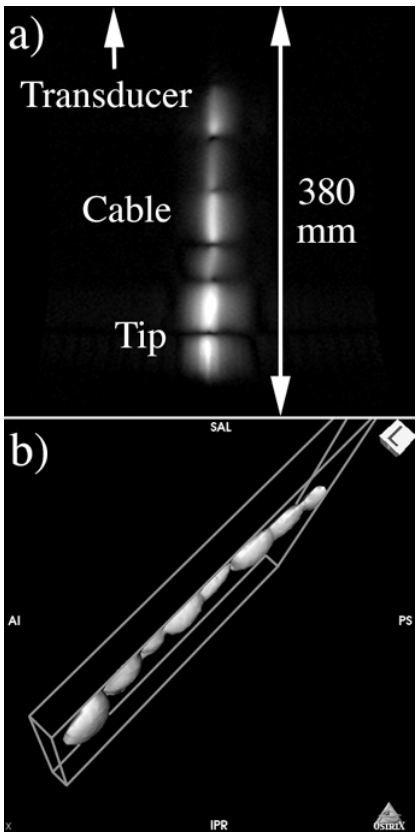

Figure 10: a) Coronal MR image of cuboid phantom; b) reception pattern reconstructed from coronal MR images.

Fig. 11 shows an axial image across the cuboid obtained using the catheter receiver, with the resolution phantom now present. The internal structure is resolved, but some small variations in brightness can be seen over its cross-section, possibly due to limited decoupling. Using a slice thickness of 5 mm and 4 excitations, 6 slices were acquired in 3 min 34 sec with an average SNR of ≈ 70 over the cross-section of the resolution phantom. This result is encouraging; however, further work is required to determine detailed performance, especially in comparison with a surface array coil.

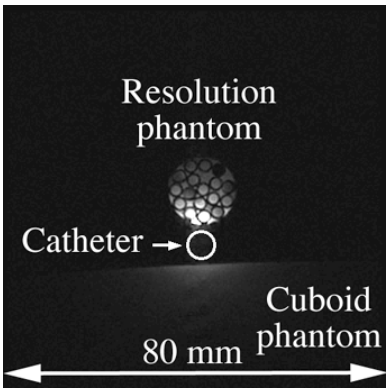

Figure 11: Axial MR image of resolution phantom.

CONCLUSIONS

Magneto-inductive catheter receivers for ^{1}H MRI in a 3 T magnetic field have been successfully demonstrated, on the basis of scaling laws derived from the design layout and the lumped-element equivalent circuit. The circuits are realized in thin-film form, and are capable of integration on a wide variety of catheters to add internal imaging and catheter visualization. Further work is clearly required to establish any SNR advantage over surface coils, and to confirm intrinsic safety and durability before *in vivo* trials can begin. This work is in progress.

ACKNOWLEDGEMENTS

The support of The Wellcome Trust is gratefully acknowledged, as the assistance of Dr Munir Ahmad.

REFERENCES

[1] P.A. Bottomley, E. Atalar, R.F. Lee, K.A. Shunk, A. Lardo, "Cardiovascular MRI probes for the outside in and for the inside out" *Magn. Reson. Mats. Phys. Biol. Med.* vol. 11, pp. 49-51, 2000.

[2] O. Ocali, E. Atalar, "Intravascular magnetic resonance imaging using a loopless catheter antenna" *Magn. Reson. Med. vol.* 37, pp. 112-118, 1997.

[3] M. Burl, G.A. Coutts, D. Herlihy, et al. "Twisted-pair RF coil suitable for locating the track of a catheter" *Magn. Reson. Med.* vol. 41, pp. 636-638, 1999.

[4] A. Surowiec, S.S. Stuchly, L. Eidus, A. Swarup, "In-vitro dielectric properties of human tissue at radio frequencies" *Phys. Med. Biol.* vol. 32, pp. 615-621, 1987.

[5] M.K. Konings, L.W. Bartels, H.F.M. Smits, C.J.G. Bakker, "Heating around intravascular guidewires by resonating RF waves" *J. Magn. Reson. Imag.* vol. 12, pp. 79-95, 2000.

[6] S. Weiss, P. Vernickel, T. Schaeffter, V. Schulz, B. Gleich, "Transmission line for improved RF safety of interventional devices" *Magn. Reson. Med.* vol. 54, pp. 182-189, 2005.

[7] A. Krafft, S. Müller, R. Umathum, W. Semmler, M. Bock, "B_1 field-insensitive transformers for RF-safe transmission lines" *Magn. Reson. Mater. Phys.* vol 19, pp. 257-266, 2006.

[8] E. Shamonina, V.A. Kalinin, K.H. Ringhofer, L. Solymar, "Magneto-inductive waveguide" *Elect. Lett. vol.* 38, pp. 371-373, 2002.

[9] R.R.A. Syms, L. Solymar, I.R. Young "Periodic analysis of MR-safe transmission lines" *IEEE J. Sel. Top. Quant.* Elect. vol. 16, pp. 433-440, 2010.

[10] Syms R.R.A., Young I.R., Solymar L., Floume T. "Thin-film magneto-inductive cables" *J. Phys. D. Appl. Phys.* vol. 43, 055102, 2010.

[11] Syms R.R.A., Young I.R., Ahmad M.M., Rea M. "Magnetic resonance imaging with linear magneto-inductive waveguides" *J. Appl. Phys.* vol. 112, 114911, 2012.

CONTACT

*R.R.A.Syms, tel: +44-207-594-6203; r.syms@ imperial.ac.uk